Quantitative phase imaging with broadband fields

Zhuo Wang[a)] and Gabriel Popescu[b)]
Department of Electrical and Computer Engineering, Quantitative Light Imaging Laboratory, Beckman Institute for Advanced Science and Technology, University of Illinois at Urbana-Champaign, Urbana, Illinois 61801, USA

(Received 21 December 2009; accepted 12 January 2010; published online 3 February 2010)

Recently, Wolf has shown that the phase measurement associated with fields that are not monochromatic, which is relevant for all x-ray structure investigations, must be properly defined via a cross-spectral density function under full spatial coherence conditions; otherwise, the problem is meaningless and has no solution [E. Wolf, Phys. Rev. Lett. **103**, 075501 (2009)]. We propose an experimental realization for retrieving the phase across the entire field of an image. The demonstration is performed using broadband optical fields, but can be extended to other electromagnetic radiation, including x-rays. *© 2010 American Institute of Physics*. [doi:10.1063/1.3304787]

In solving the inverse scattering problem using x-rays (or other electromagnetic radiation), the phase of the scattered field is of essence, as it reports on the structure function of the object,

$$S(\mathbf{q}) = \sum_j e^{\mathbf{q}\cdot\mathbf{r}_j}, \quad (1)$$

where $\mathbf{q}$ is the wave vector, and $\mathbf{r_j}$ is the position vector of the j$^{\text{th}}$ scatterer, or atom in the case of x-rays scattering from crystals. Thus, measurements of irradiance loose this structural information. Very recently, it has been shown that, if a nonmonochromatic field is spatially coherent, the phase information is that of an effective monochromatic field oscillating at the average frequency.[1]

Here, we propose a general experimental approach for retrieving the phase information over the entire image obtained with a broadband field. In optics, quantitative phase imaging has become a dynamic field, especially due to its potential for nanoscale cell and tissue imaging.[2] Note that knowledge of the phase in the image plane as defined by an imaging system, allows reconstructing the field in the far field zone with very high accuracy.[3] Our experimental demonstration, which follows the theoretical solution proposed by Wolf,[1] was performed with optical fields, but the scheme is generally applicable to other electromagnetic fields, including x-rays.

The principle relies on the spatial decomposition of a statistically homogeneous field U into its *spatial average* (i.e., unscattered) and a *spatially varying* (scattered) component

$$U(\mathbf{r};\omega) = U_0(\omega) + U_1(\mathbf{r};\omega) = |U_0(\omega)|e^{i\phi_0(\omega)} + |U_1(\mathbf{r};\omega)|e^{i\phi_1(\mathbf{r};\omega)}, \quad (2)$$

where $\mathbf{r}=(x,y)$. Here the field is assumed to be *fully spatially coherent*.

Using the spatial Fourier representation $\tilde{U}(\mathbf{q};\omega)$ of U, it becomes apparent that the average field U_0 is proportional to the dc component $\tilde{U}(\mathbf{0};\omega)$, whereas U_1 describes the nonzero frequency content of U. Thus, the image field U can be regarded as the interference between its spatial average and its spatially-varying component. The description of an arbitrary image as an interference phenomenon has been recognized more than a century ago by Abbe in the context of microscopy as follows: "the microscope image is the interference effect of a diffraction phenomenon."[4] Further, describing an image as an (complicated) interferogram set the basis for Gabor's[5] development of holography. The cross-spectral density can be written as

$$W_{01}(\mathbf{r};\omega) = \langle U_0(\omega)\cdot U_1^*(\mathbf{r};\omega)\rangle, \quad (3)$$

where the angular brackets denote ensemble average and * stands for complex conjugation. If ω_0 is the mean frequency of the power spectrum $S(\omega)=\langle|U_0(\omega)|^2\rangle$, W has the factorized form

$$W_{01}(\mathbf{r};\omega-\omega_0) = |W_{01}(\mathbf{r};\omega-\omega_0)|e^{i[\Delta\phi(\mathbf{r};\omega-\omega_0)]}. \quad (4)$$

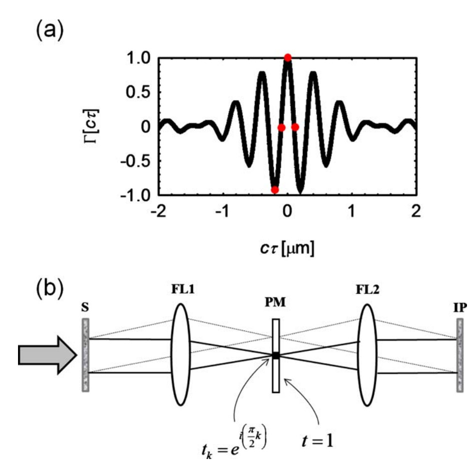

FIG. 1. (Color online) (a) The autocorrelation function Γ. The four dots indicate the phase shifts produced by PM. The refractive index of the medium is 1.33. (b) Experimental setup: S specimen, FL Fourier lenses, PM phase modulator, IP image plane. The transmission functions for the unscattered field (t_k) and scattered field (t) are indicated.

[a)]Electronic mail: zwang47@illinois.edu.
[b)]Electronic mail: gpopescu@illinois.edu.

 © 2010 American Institute of Physics

Author complimentary copy. Redistribution subject to AIP license or copyright, see http://apl.aip.org/apl/copyright.jsp

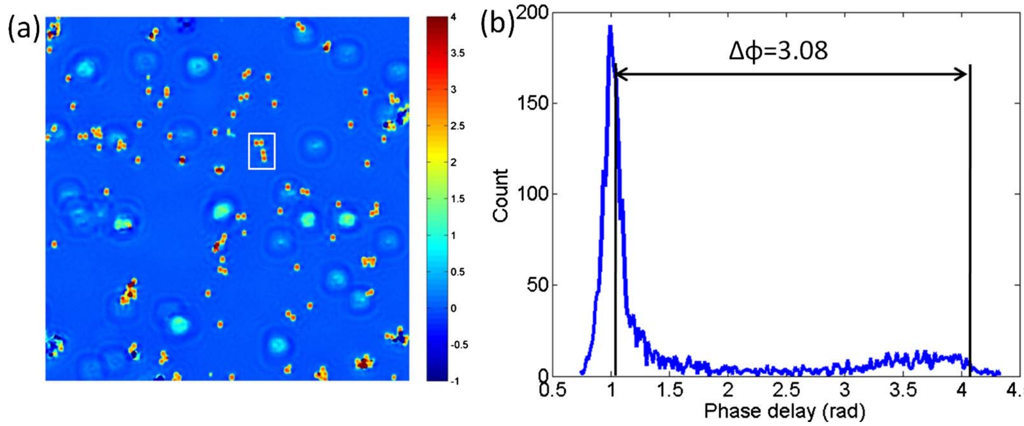

FIG. 2. (Color online) (a) Quantitative phase image of 1 μm diameter polystyrene beads. Color bar indicates phase in radians. (b) Histogram of the selected area of (a). The average phase shift through beads is shown. Fig. 1 is single column; Fig. 2 is double column.

It follows that the temporal cross-correlation function is obtained by Fourier transforming Eq. (4),[6]

$$\Gamma_{01}(\mathbf{r};\tau) = |\Gamma_{01}(\mathbf{r};\tau)| \cdot e^{i[\omega_0\tau+\Delta\phi(\mathbf{r};\tau)]}, \quad (5)$$

with $\Delta\phi(\mathbf{r})=\phi_0-\phi_1(\mathbf{r})$ the spatially varying phase difference of the cross-correlation function. Equation (4) indicates that, for spatially coherent illumination, the spatially varying phase of the cross-correlation function can be retrieved through measurements at various time delay τ. This phase information is equivalent to that of a purely monochromatic light at frequency ω_0. Using Eq. (5), one obtains the following irradiance distribution in the plane of interest as a function of the time delay τ:

$$I(\mathbf{r};\tau) = I_0 + I_1(\mathbf{r}) + 2|\Gamma_{01}(\mathbf{r};\tau)|\cos[\omega_0\tau + \Delta\phi(\mathbf{r})]. \quad (6)$$

When one varies the delay τ between U_0 and U_1, interference is obtained simultaneously at each point of the image. The average U_0 is constant over the entire plane and can be regarded as the common reference field of an array of interferometers. In addition, U_0 and U_1 traverse similar optical paths. Thus, the influence of inherent phase noise due to vibration or air fluctuations is inherently minimized, allowing for a precise retrieval of $\Delta\phi$.

For modifications of the time delay around $\tau=0$ that are comparable to the optical period, $|\Gamma|$ can be assumed to vary slowly at each point. Thus, using Eq. (6), the spatially varying phase of Γ can be reconstructed as

$$\Delta\phi(\mathbf{r}) = \arg\left[\frac{I(\mathbf{r};\tau_3) - I(\mathbf{r};\tau_1)}{I(\mathbf{r};\tau_0) - I(\mathbf{r};\tau_2)}\right], \quad (7)$$

where τ_k is given by $\omega_0\tau_k=k\pi/2$, $k=0,1,2,3$. If we define $\beta(\mathbf{r})=|U_1(\mathbf{r})|/|U_0|$, then the phase associated with the image field $U=U_0+U_1$ can be determined as

$$\phi(\mathbf{r}) = \arg\left\{\frac{\beta(\mathbf{r})\sin[\Delta\phi(\mathbf{r})]}{1+\beta(\mathbf{r})\cos[\Delta\phi(\mathbf{r})]}\right\}. \quad (8)$$

Equation (8) shows how the quantitative phase image is retrieved via four successive intensity images measured for each phase shift.

In our experiment, we used a broadband, spatially coherent field. Figure 1(a) shows the autocorrelation function of the field, $\Gamma(c\tau)$, with c the speed of light, which was inferred by taking the Fourier transform of a measured spectrum. Note that the sinusoid indicates the equivalent monochromatic wave associated with this spatially coherent field. Lens FL generates the spatial Fourier transform of the field at its back focal plane, where the phase modulator PM (a liquid crystal modulator in our case) shifts the phase of the unscattered light in increments of $\pi/2$. Fourier lens FL2 generates the resulting image at the image plane IP. In our experiments, the experimental setup was implemented via a phase contrast microscope, which allows for high resolution images, $\sim$0.35 μm transverse resolution using a 0.75 numerical aperture objective. The illumination field was the white light produced by a halogen lamp, which is typically used in phase contrast microscopes.

Four images associated with the individual phase shifts were recorded and combined as described in Eqs. (7) and (8) to obtain a quantitative phase image. Figure 2 shows an example of such an image and demonstrates the principle of phase retrieval using broadband fields. Polystyrene beads of 1 μm in diameter immersed in water were imaged by our system. The quantitative phase map is shown in Fig. 2(a) and the histogram of phase shifts in Fig. 2(b). The maximum phase shift through the beads ($n=1.59$) with respect to surrounding medium (water, $n_w=1.33$) is expected to be $\delta\phi=(2\pi/\lambda_0)\Delta nd$, with $\lambda_0=\omega_0/c$, $\Delta n=n-n_w$, and $d=1$ μm. Thus, the measured value of 3.08 compares very well with the expected $\delta\phi=3.07\pm0.15$, where the error is due to the size distribution provided by the manufacturer.

In summary, we developed an experimental approach to retrieve quantitative phase images with broadband fields, which can be applied in principle to all electromagnetic radiation. In the x-ray field, recent efforts have lead to generating spatially coherent fields.[7,8] Implementing an efficient method for generating Fourier transforms and phase shifting is more challenging than in the optical regime,[9] but perhaps achievable in the near future.

This research was supported in part by NSF CAREER under Grant No. 08-46660 and Grainger Foundation.

[1]E. Wolf, Phys. Rev. Lett. **103**, 075501 (2009).
[2]G. Popescu, in *Methods in Cell Biology*, edited by P. J. Bhanu (Elsevier, Burlington, MA, 2008), Vol. 90, p. 87.
[3]H. Ding, Z. Wang, F. Nguyen, S. A. Boppart, and G. Popescu, Phys. Rev. Lett. **101**, 238102 (2008).
[4]F. Zernike, Physica (Amsterdam) **9**, 686 (1942).

Author complimentary copy. Redistribution subject to AIP license or copyright, see http://apl.aip.org/apl/copyright.jsp

[5]D. Gabor, Nature (London) **161**, 777 (1948).
[6]L. Mandel and E. Wolf, *Optical Coherence and Quantum Optics* (Cambridge University Press, Cambridge, New York, 1995).
[7]D. T. Attwood, *Soft X-Rays and Extreme Ultraviolet Radiation: Principles and Applications* (Cambridge University Press, Cambridge, UK; New York, 2000).
[8]R. Cerbino, L. Peverini, M. A. C. Potenza, A. Robert, P. Bösecke, and M. Giglio, Nat. Phys. **4**, 238 (2008).
[9]B. Cederström, R. N. Cahn, M. Danielsson, M. Lundqvist, and D. R. Nygren, Nature (London) **404**, 951 (2000).

Author complimentary copy. Redistribution subject to AIP license or copyright, see http://apl.aip.org/apl/copyright.jsp